



CHORUS

This is the accepted manuscript made available via CHORUS. The article has been published as:

Closed-Loop Control of Complex Networks: A Trade-Off between Time and Energy

Yong-Zheng Sun, Si-Yang Leng, Ying-Cheng Lai, Celso Grebogi, and Wei Lin

Phys. Rev. Lett. **119**, 198301 — Published 7 November 2017

DOI: [10.1103/PhysRevLett.119.198301](https://doi.org/10.1103/PhysRevLett.119.198301)

Closed-loop control of complex networks: A trade-off between time and energy

Yong-Zheng Sun,^{1,2} Si-Yang Leng,^{1,3,4} Ying-Cheng Lai,⁵ Celso Grebogi,⁶ and Wei Lin^{1,3,*}

¹*Center for Computational Systems Biology of ISTBI, Fudan University, Shanghai 200433, China*

²*School of Mathematics, China University of Mining and Technology, Xuzhou 221116, China*

³*School of Mathematical Sciences and LMNS, Fudan University, Shanghai 200433, China*

⁴*Collaborative Research Center for Innovative Mathematical Modelling,
Institute of Industrial Science, The University of Tokyo, Tokyo 153-8505, Japan*

⁵*School of Electrical, Computer, and Energy Engineering,
Arizona State University, Tempe, Arizona 85287-5706, USA*

⁶*Institute for Complex Systems and Mathematical Biology,
University of Aberdeen, Aberdeen AB24 3UE, UK*

Controlling complex nonlinear networks is largely an unsolved problem at the present. Existing works focused either on open-loop control strategies and their energy consumptions, or on closed-loop control schemes with an infinite-time duration. We articulate a finite-time, closed-loop controller with an eye toward the physical and mathematical underpinnings of the trade-off between control time and energy as well as their dependence on the network parameters and structure. The closed-loop controller is tested on a large number of real systems including stem cell differentiation, food webs, random ecosystems, and spiking neuronal networks. Our results represent a step forward in developing a rigorous and general framework to control nonlinear dynamical networks with a complex topology.

Recent years have witnessed a growth of interest in controlling complex networks. A vast majority of the existing works in this area dealt with the controllability and control of linear dynamical networks [1–25, 65, 66]. Controlling complex networks with nonlinear dynamics has been limited to brute force strategies such as local pinning [28–31] or to specific systems exhibiting a simple kind of multistability [32–36]. Most existing methods of controlling nonlinear networks were of the open-loop type, i.e., one selects a suitable subset of nodes and applies *pre-defined* control signals or parameter perturbations, which are state independent, to drive the system from an initial state to a desired target. It is, however, difficult to formulate a general and robust open-loop control framework. It is thus of interest to investigate closed-loop control for complex nonlinear dynamical networks, in which a pre-designed feedback loop generates control signals according to the instantaneous state of the system. Closed-loop control thus provides a theoretically relevant and a significant alternative to controlling complex nonlinear networks.

In controlling chaos in low-dimensional dynamical systems, both open- and closed-loop controls were extensively investigated. The OGY (Ott-Grebogi-Yorke) [37] principle, in which small, deliberate, and time dependent perturbations calculated from measured time series are applied to a parameter or a dynamical variable to keep the system in the vicinity of a target periodic orbit, belongs to the open-loop category. Because of the hallmark of chaos, i.e., sensitive dependence on initial conditions, the control perturbation can be small and there is great flexibility to switch the target orbit. However, real-time observations of the system are needed and control can be fragile to external disturbances. The method of Pyragas [38, 39] is a closed-loop type of control in which a de-

layed feedback term is added to the system equations. It does not require real-time observation and analysis of the system so that experimental implementation is greatly facilitated and control can be robust against noise, but the time for control realization is infinite and control flexibility is limited. The developmental history of the field of chaos control provides another motivation for us to consider frameworks as alternative to open-loop methods for nonlinear network control.

In this Letter, we articulate and analyze a global, finite-time and closed-loop control framework for complex nonlinear dynamical networks. To ensure that our framework is physically significant, we focus on the control energy and the time required to achieve control, and investigate their trade-off. We study how network parameters and structure affect the control time and energy, and test the control framework using a variety of real biophysical systems including stem cell differentiation, food webs, random ecosystems, and neuronal networks. Analytically, we derive rigorous upper bounds for both the control energy and time. These results suggest that to develop closed-loop control with optimized control time and energy not only is fundamental to the network control field, but also has applied values.

We consider nonlinear dynamical networks described by $\dot{x}_i = f(x_i) + \sum_{j=1}^N c_{ij} \Gamma x_j(t) + \mathbf{u}[\mathbf{x}(t)]B_i$, $1 \leq i \leq N$, where N is the network size, $x_i = [x_{i1}, \dots, x_{id}]^\top \in \mathbb{R}^d$ denotes the d -dimensional state variable of the i -th node, \mathbf{x} represents the state variables of the whole network, $f : \mathbb{R}^d \rightarrow \mathbb{R}^d$ is a nonlinear velocity field governing the nodal dynamics and satisfying $\|f(x)\| \leq l\|x\|$ or $|x^\top f(x)| \leq l\|x\|$ ($\forall x \in \mathbb{R}^d$) with a positive constant l , $\mathbf{C} = (c_{ij}) \in \mathbb{R}^{N \times N}$ is the coupling matrix determined by the network structure, $\Gamma \in \mathbb{R}^{d \times d}$ describes the internal coupling configuration at each node, $\mathbf{u}[\mathbf{x}(t)] =$

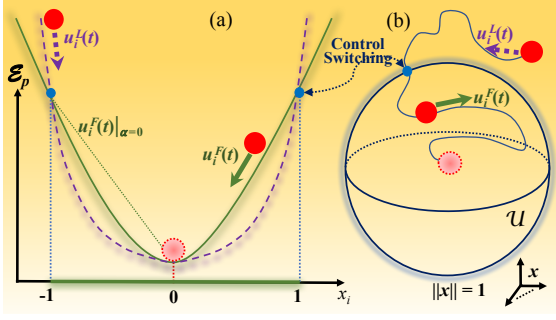


FIG. 1. Physical underpinning of our closed-loop feedback controller. (a) System moving according to the potential function $\mathcal{E}_p^{L,F}$ (dashed curves) underlying closed-loop feedback controllers $u_i^{L,F}$, where u_i^L specifies a linear feedback controller that acts outside of the unit sphere, and u_i^F denotes a general feedback controller that is activated once the system is inside the unit sphere. (b) Controlled system trajectory in the phase space by u_i^S , where a control switch occurs when the system crosses the unit sphere $\|\mathbf{x}\| = 1$.

$[u_i(t)]_{1 \leq i \leq M} \in \mathbb{R}^{d \times M}$ ($M \leq N$) is the closed-loop control protocol to be designed, and $B_i = [b_{i1}, \dots, b_{iM}]^\top \in \mathbb{R}^M$ ($b_{im} = 0, 1$) characterizes the driving by the controller \mathbf{u} to the i -th node. Going beyond the existing works on open-loop control of complex networks, where the goal is to drive the system to an instantaneous state, we set the control target to be an *unstable* steady state, which, for mathematical convenience, is assumed to be $x_i = 0$ for all i . For any nontrivial target state, a direct translation can be used to transfer the state to $x_i = 0$.

For a general nonlinear dynamical system, a straightforward approach to realizing closed-loop control [40–42] is to set each component of \mathbf{u} as $u_i = -kx_i \triangleq u_i^L$ ($1 \leq i \leq M \leq N$). In principle, this linear feedback controller of strength k is able to steer the dynamics to converge to the target $x_i = 0$, but the time required for convergence is *infinite*. We thus seek alternative methods [43–46] to achieve finite control time and robustness against disturbances. A typical form of the feedback controller is $u_i = -k \text{sig}(x_i)^\alpha \triangleq u_i^F$, which can drive the system to $x_i = 0$ for all $t \geq T_f^F$ with $T_f^F < \infty$, where $\text{sig}(x_i)^\alpha = [\text{sign}(x_{i1})|x_{i1}|^\alpha, \dots, \text{sign}(x_{id})|x_{id}|^\alpha]^\top$, $\text{sign}(\cdot)$ is a sign function, k is the control strength, and $\alpha \in (0, 1)$ is the steepness exponent. The mathematical underpinning of the controller u_i^F lies in that the non-Lipschitzian $|\cdot|^\alpha$ at $x_i = 0$ violates the solution uniqueness of the system of coupled differential equations.

To gain physical insights into the control process, we consider the potential function: $\mathcal{E}_p^{L,F}(x_i) = \int_0^{x_i} u_i^{L,F} dx_i$, which can be determined from the closed-loop feedback controller. We find that u_i^L is located higher than u_i^F for $|x_i| > 1$, while the opposite occurs for $|x_i| < 1$, as shown in Fig. 1(a). On the potential landscape, the controlled system trajectory can be regarded as a particle moving along some optimal path towards the target $x_i = 0$, the

minimum of the potential. The particle experiences a stronger potential force along a path determined by u_i^L (u_i^F) for $|x_i| > 1$ ($|x_i| < 1$). The maximum force occurs for $|x_i| < 1$ and $\alpha \rightarrow 0$. In this case, $u_i^F|_{\alpha=0}$ corresponds to a double-valued and closed-loop controller, similar to the classical bang-bang control [47]. *The basic principle is then to design two controllers in complementary regions of the phase space.* This consideration leads us to propose the following global, compound controller: $u_i = u_i^F \mathcal{I}_{\mathcal{U}} + u_i^L \mathcal{I}_{\mathcal{U}^c} \triangleq u_i^S$, where $1 \leq i \leq M$, the unit ball is defined by $\mathcal{U} = \{\|\mathbf{x}\| < 1\}$, $\mathbf{x} = [x_1^\top, \dots, x_N^\top]^\top$, $\|\cdot\|$ denotes an appropriate norm of the underlying vector, \mathcal{U}^c is the complement of \mathcal{U} , and \mathcal{I} is the indication function for a given subscript set. The norm can be taken as the L_p or L_∞ . To be representative and without loss of generality, we study the L_2 norms. As shown in Fig. 1(b), the compound controller u_i^S switches from u_i^L to u_i^F when the system enters the unit sphere.

We now prove that the controller $\mathbf{u}^S = [u_i^S]_{1 \leq i \leq M}$ enables finite-time control, and provide an estimate of T_f^S , the time required to achieve control. To be concrete, we set $M = N$, $b_{ii} = 1$, and $b_{im} = 0$ for $i \neq m$. As shown in Fig. 1(b), for $\mathbf{x}(0) \notin \mathcal{U}$, the control protocol is set as $u_i^S = u_i^L$. A direct calculation gives $d\|\mathbf{x}(t)\|^2/dt \leq -2(k-l-\eta_{\max})\|\mathbf{x}(t)\|^2$, where η_{\max} is the maximal eigenvalue of the matrix $\mathbf{H} \equiv [(\mathbf{C} \otimes \mathbf{\Gamma})^\top + \mathbf{C} \otimes \mathbf{\Gamma}]/2$, and \otimes represents the Kronecker product for matrices. Setting $k > l + \eta_{\max}$ when the networked system is outside of the ball \mathcal{U} , we get the time instant t^* such that $\mathbf{x}(t)|_{t=t^*}$ hits the sphere of \mathcal{U} with $t^* \leq [\ln \|\mathbf{x}(0)\|]/\rho$ and $\rho \triangleq k - l - \eta_{\max} > 0$. Once the orbit $\mathbf{x}(t)$ enters \mathcal{U} after t^* , because of the dissipation inside \mathcal{U} (see Supplementary Information [48]), the system will never leave it so that u_i^S becomes u_i^F with the corresponding value k for $t > t^*$, as shown in Fig. 1(b). Dynamical systems theory [48] stipulates that $d\|\mathbf{x}(t)\|^2/dt \leq -2\rho\|\mathbf{x}(t)\|^{1+\alpha}$ for $t \geq t^*$ and that $\mathbf{x}(t) \equiv 0$ for all $t \geq t^* + 1/\rho(1-\alpha)$. An analogous analysis applies to the case $\mathbf{x}(0) \in \mathcal{U}$ with $u_i^S = u_i^F$. The upper bound for T_f^S is then given by

$$T_f^{S_{\text{up}}} = \begin{cases} \frac{1}{\rho} \left[\ln \|\mathbf{x}(0)\| + \frac{1}{1-\alpha} \right], & \mathbf{x}(0) \notin \mathcal{U}, \\ \|\mathbf{x}(0)\|^{1-\alpha} \frac{1}{\rho(1-\alpha)}, & \mathbf{x}(0) \in \mathcal{U}, \end{cases} \quad (1)$$

with the condition $\rho > 0$. We see that, for given values of α and $\mathbf{x}(0)$ as well as specific network dynamics with l , \mathbf{C} and $\mathbf{\Gamma}$, the estimation (1) is on the order $O(1/k)$, where $O(1)$ is a positive and bounded quantity. Accordingly, \mathbf{u}^S with a larger value of k can expedite control.

For our controller \mathbf{u}^S , the required energy cost is [7] $\mathcal{E}_c^S = \int_0^{T_f^S} \sum_{i=1}^N \|u_i^S(t)\|^2 dt$. A lengthy calculation [48] leads to the following upper bound for the energy cost

$$\mathcal{E}_c^{S_{\text{up}}} = \begin{cases} k^2 \frac{1}{2\rho} \left[1 - \|\mathbf{x}(0)\|^{-2} + \frac{2\zeta}{1+\alpha} \right], & \mathbf{x}(0) \notin \mathcal{U}, \\ k^2 \frac{\zeta}{\rho(1+\alpha)} \|\mathbf{x}(0)\|^{1+\alpha}, & \mathbf{x}(0) \in \mathcal{U}, \end{cases} \quad (2)$$

where $\zeta = (Nd)^{1-\alpha}$. Since $\rho \sim k$, \mathcal{E}_c^S is bounded from

above by a quantity on the order of $O(k)$. This indicates that, for a given network and given values of α and $\mathbf{x}(0)$, increasing k will raise the energy cost. In addition, for fixed values of α and $\mathbf{x}(0)$, if k is sufficiently large, increasing l or η_{\max} will lead to larger upper bounds for both the control time and energy. For example, for an unweighed and undirected network with $\mathbf{\Gamma}$ being an identity matrix, the quantity η_{\max} becomes $\lambda_{\max}(\mathbf{C})$, so increasing the maximum eigenvalue would demand more time and energy for the \mathbf{u}^S driven control to be successful.

Using $\partial_\alpha(\ln T_f^{S_{\text{up}}}) = \ln \|\mathbf{x}(0)\|^{-1} + 1/(1-\alpha)$, $\|\mathbf{x}(0)\| \leq 1$, and $\alpha \in (0, 1)$, we can prove that $T_f^{S_{\text{up}}}$ is an increasing function of α , i.e., $\partial_\alpha(T_f^{S_{\text{up}}}) > 0$, implying that control can be expedited by using a smaller value of the steepness exponent α . In addition, the condition $\partial_\alpha(\mathcal{E}_c^{S_{\text{up}}}) < 0$ implies that smaller values of α lead to higher energy costs. The dependence of the energy on α is consistent with the intuitive, potential-landscape based physical scenario of control. These results reveal a trade-off between the control time and energy cost for our controller \mathbf{u}^S with respect to variations in α or k . For example, consider the index $\mathcal{J}_{\gamma,\beta}(k) = \gamma[T_f^S] + \beta[\mathcal{E}_c^S]$, where γ and β are adjustable weights determined by the specific system and $[\cdot]$ is a normalization function. Since $\mathcal{J}_{\gamma,\beta}(k) \sim O(1/k) + O(k)$, there must exist a number $k_c \gtrsim l + \eta_{\max}$ at which the quantity $\mathcal{J}_{\gamma,\beta}$ reaches its minimum. The optimal control strength is thus given by $k = k_c$ in the sense that control can be achieved in less time with lower energy cost in terms of the index $\mathcal{J}_{\gamma,\beta}$.

We demonstrate the working of our optimal closed-loop controller \mathbf{u}^S , its superior performance as compared with the conventional controllers $\mathbf{u}^L = [u_i^L]_{1 \leq i \leq M}$, and the corresponding analytic bounds of the control time and energy, using a number of representative real-world complex nonlinear dynamical networks.

Controlling stem cell fate. We demonstrate that our closed loop controller can drive two different cell fates to the critical expression level to enable stem cells to remaster their cell fate for cellular differentiation. Specifically, we consider the following network model for hematopoietic stem cells [49], which describes the interaction between two suppressors during cellular differentiation for neutrophil and macrophage cell fate choices [50, 51]: $\dot{x}_1 = 0.5 - x_1$, $\dot{x}_2 = 5x_1/[(1+x_1)(1+x_3^4)] - x_2$, $\dot{x}_3 = 5x_4/(1+x_4)(1+x_2^4) - x_3$, $\dot{x}_4 = 0.5/(1+x_2^4) - x_4$, $\dot{x}_5 = [x_1x_4/(1+x_1x_4) + 4x_3/(1+x_3)]/(1+x_2^4) - x_5$, $\dot{x}_6 = [x_1x_4/(1+x_1x_4) + 4x_2/(1+x_2)]/(1+x_3^4) - x_6$, where $x_{2,3}$ are the expression levels of two lineage-specific counter-acting suppressors Gfi-1 and Egr(1,2), which are activated by their transcription factors $x_{1,4}$ and simultaneously regulate the downstream genes $x_{5,6}$, respectively. As specified in Fig. 2, the system has three steady states: $U_{1,2,3}$, where $U_{1,3}$ correspond to different cell fates and are stable, and U_2 represents a critical expression level connecting the two fates and is unstable. Figure 2(a)

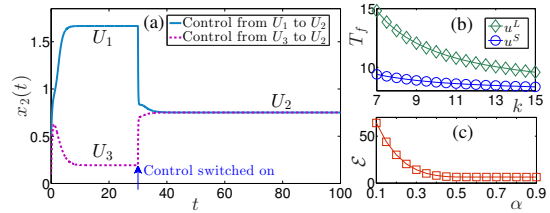


FIG. 2. Controlling a cellular differentiation network model from the steady state $U_1 = (0.5, 1.66, 0.03, 0.06, 0.02, 2.53)$ or $U_3 = (0.5, 0.19, 1.66, 0.50, 2.69, 0.10)$ to the steady state $U_2 = (0.5, 0.75, 1.05, 0.38, 1.69, 0.83)$. (a) Uncontrolled dynamics [for $t \in [0, 30]$] and controlled dynamics (for $t \geq 30$) for the expression levels of suppressor x_2 , where $k = 10$ and $\alpha = 0.5$ when u^S is switched on. (b) For $\alpha = 0.5$, control time versus k for the two controllers $u^{S,L}$. (c) For $k = 10$, control energy versus α for controller u^S .

shows that initially x_2 of the uncontrolled system converges to the stable steady state U_1 or U_3 . From $t = 30$, we apply the finite time controller $u^S = u^F \mathcal{T}_U + u^L \mathcal{T}_{U^c}$ with $\mathcal{U} = \{\|\mathbf{x} - U_2\| < 1\}$, $u^L = -k(x_2 - U_{22})$ and $u^F = -k \cdot \text{sign}(x_2 - U_{22}) \cdot |x_2 - U_{22}|^\alpha$ to x_2 , which is the only variable experimentally accessible [49]. Here, U_{22} is the second component of U_2 . The controlled system in either of the stable states is driven rapidly to the critical state U_2 , indicating that a finite-time, closed-loop intervention can make the stem cells remaster their cell fate for cellular differentiation. Further, for sufficiently strong control strength k , the converging time with the controller u^S is shorter than that with u^L , as shown in Fig. 2(b). Figure 2(c) shows, for a fixed value of k , the required control energy decreases with the steepness exponent α , as predicted by our analysis.

Controlling nonlinear ecosystems on food-web networks. The nonlinear ecological model is described by $\dot{x}_i = x_i(1 - x_i/K_i)(x_i/A_i - 1) \triangleq f(x_i)$, where x_i is the species abundance, f characterizes the logistic growth, and the carrying capacity is K_i . The model includes the Allee effect, where the species is *destined for extinction* if its abundance is lower than a threshold value ($x_i < A_i$) [52–54]. We demonstrate that our control method can successfully restore the system out of extinction to a sustainable state. In particular, for each i , the model has two stable steady states ($x_i = 0$, K_i , corresponding to species extinction and capacity overload, respectively), and one unstable steady state ($x_i = A_i$). To prevent the system from evolving into one of the stable steady state, we choose the control target to be $x_i = A_i$ for all i that represents restoration or sustainment of species to a state with moderate abundance. The coupling matrices \mathbf{C} are constructed from a large number of real food-web networks [48]. For the three controllers $\mathbf{u}^{S,F,L}$, we calculate the respective control time $T_f^{S,F,L}$ required to drive the system into the neighborhood of the target: $|x_i(t) - A_i| \leq 10^{-4}$, $1 \leq i \leq N$. The controller

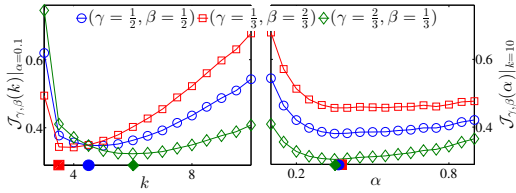


FIG. 3. Dependence of optimal control strength or steepness exponent on preferential weights. For the Florida food web, optimal locations of the control indices $\mathcal{J}_{\gamma,\beta}(k)|_{\alpha=0.1}$ and $\mathcal{J}_{\gamma,\beta}(\alpha)|_{k=10}$ versus the weights, as indicated by the markers along the horizontal axis.

\mathbf{u}^S results in the least control time (see Tab. S1 in [48] for detailed values from all 22 food-web networks).

To verify our analytic prediction of optimal control through the control indices $\mathcal{J}_{\gamma,\beta}$, we use the Florida food web [48] and calculate the indices as a function of k or α . Figure 3 shows that the optimal values of k_c and α_c depend on the combination of the preferential weights (γ, β) , which agree well with the respective analytic results. Simulations further reveal that the optimal value k_c is more sensitive to the choice of the preferential weights than α_c , which is reasonable as decreasing the control time tends to make the value of k_c larger.

Controlling complex random ecosystems. Consider a general ecosystem described by $\dot{\mathbf{x}} = \mathbf{C}\mathbf{x}$, where each species x_i is one-dimensional, $\mathbf{C} = (c_{ij})_{N \times N}$ describes the random mutual interactions with $c_{ii} = -r$, and N is the population size. Three types of random matrices \mathbf{C} were studied extensively, which correspond to three typical ecosystems: (a) *May's classic ecosystem* [55] where, with probability P , the off-diagonal elements c_{ij} are set as mutually independent Gaussian random variables $\mathcal{N}(0, \sigma_0^2)$ and the probability for the elements to be zero is $(1 - P)$, (b) *a mixed ecosystem of competition and mutualism* [56] where the off-diagonal elements c_{ij} and c_{ji} have the same sign, which are drawn from the distribution $(\pm|\mathcal{Y}|, \pm|\mathcal{Y}|)$ with probability P and are zero with probability $(1 - P)$, and (c) *the predator-prey (PP) ecosystem* [56] where c_{ij} and c_{ji} have the opposite signs and are from the distribution $(\pm|\mathcal{Y}|, \mp|\mathcal{Y}|)$. As either N or the variance of \mathbf{C} 's elements increases, all three ecosystems eventually become unstable, reflecting the instability of certain steady state in the original ecosystem from which the linear random system was derived [55, 56].

We employ \mathbf{u}^S to control the ecosystems, which becomes a particular case of our general nonlinear network control framework with $l = 0$, $\mathbf{\Gamma} = \mathbf{1}$, $b_{ii} = 1$ and all other $b_{im} = 0$. To achieve finite-time control, we estimate the maximal eigenvalue η_{\max} of $\mathbf{H} = (\mathbf{C}^\top + \mathbf{C})/2$ (see SI). For May's classic ecosystem, the well-known semicircle law for random matrices stipulates that \mathbf{H} 's eigenvalues are located in $[-\sqrt{2NP}\sigma_0 - r, \sqrt{2NP}\sigma_0 - r]$ as $N \rightarrow \infty$ (SI). According to Eq. (1), to realize finite-time control

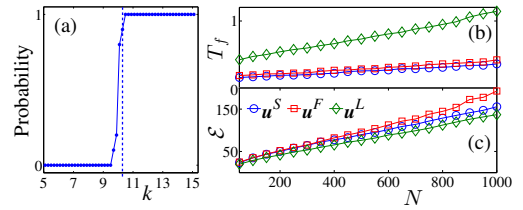


FIG. 4. For May's classic ecosystems, the probability of successful control versus k (a), where the vertical dashed line corresponds to η_{\max} , $N = 250$, $P = 0.25$, $\sigma_0 = 1$, $r = 1$, and $\alpha = 0.6$, and required control time cost (b) and energy cost (c), respectively, with the increase of N for $k = 1.1\eta_{\max}$.

requires $k > \eta_{\max} = \sqrt{2NP}\sigma_0 - r$ (Condition-A). As shown in Fig. 4(a), successful control is achieved for sufficiently large values of k . However, from the estimates of the control time and energy [Eqs. (1) and (2), respectively], we see that, for a fixed large value of k , an increase in either N or σ_0 slows down the control and consume more energy, eventually violating Condition-A and causing the control to fail, as shown in Figs. 4(b)-4(c). While the controller \mathbf{u}^S requires the least control time among the three available controllers, for large system size the corresponding energy cost is not necessarily minimum.

For the mixed ecosystem with $\mathcal{Y} \sim \mathcal{N}(0, \sigma_0^2)$, from \mathbf{H} 's eigenvalues distribution obtained in [48], we have $k > \sqrt{2NP}(1 + 2/\pi)\sigma_0 - r$ (Condition-B) that ensures finite-time control in the probabilistic sense. Similarly for the PP system, we require $k > \sqrt{2NP}(1 - 2/\pi)\sigma_0 - r$ (Condition-C). Overall, the Conditions A-C reveal a *hierarchy* where the PP, May's classic, and mixed ecosystems require the weakest, intermediate, and strongest control strength k . The control time for the three systems can be made finite and identical because the respective choices of the k value can result in the same value of ρ in Eq. (1). In spite of this, the ordering of the control energy for the three types of ecosystems cannot be altered because k appears still in Eq. (2) in addition to ρ .

Akin to the previous example of controlling stem cell fate via only one suppressor, we apply our finite-time controller to different numbers of species in the ecosystem with an undirected scale-free coupling matrix \mathbf{C} , which reveals a high flexibility of our controller (see [48]).

To summarize, we develop a closed-loop control framework for nonlinear dynamical networks to drive the system to a desired unstable steady state in finite time and with predictable energy. Because of the closed-loop nature and high flexibility of the controller, it is suitable for experimental control of nonlinear networks. We obtain physical and mathematical understandings of the trade-off between control time and energy. Our closed-loop controller is also effective for realizing synchronization in nonlinear neuronal networks (see [48]). While the issue of optimal energy associated with closed-loop control and single- or two-layer structure has been inves-

tigated [57, 58], prior to our work a closed-loop control scheme for nonlinear dynamical networks with both optimal time and energy had not been achieved. Our work provides a base for developing a general, physically realizable closed-loop control scheme for complex nonlinear networks with completely unknown steady states.

WL is supported by the NSFC (Grants No. 11322111 and No. 61773125). YZS is supported by the NSFC (Grant No. 61403393). YCL would like to acknowledge support from the Vannevar Bush Faculty Fellowship program sponsored by the Basic Research Office of the Assistant Secretary of Defense for Research and Engineering and funded by the Office of Naval Research through Grant No. N00014-16-1-2828. YZS and SYL contribute equally to the work.

* wlin@fudan.edu.cn

- [1] A. Lombardi and M. Hörnquist, *Phys. Rev. E* **75**, 056110 (2007).
- [2] B. Liu, T. Chu, L. Wang, and G. Xie, *IEEE Trans. Automat. Contr.* **53**, 1009 (2008).
- [3] A. Rahmani, M. Ji, M. Mesbahi, and M. Egerstedt, *SIAM J. Contr. Optim.* **48**, 162 (2009).
- [4] Y.-Y. Liu, J.-J. Slotine, and A.-L. Barabási, *Nature (London)* **473**, 167 (2011).
- [5] W.-X. Wang, X. Ni, Y.-C. Lai, and C. Grebogi, *Phys. Rev. E* **85**, 026115 (2012).
- [6] J. C. Nacher and T. Akutsu, *New J. Phys.* **14**, 073005 (2012).
- [7] G. Yan, J. Ren, Y.-C. Lai, C.-H. Lai, and B. Li, *Phys. Rev. Lett.* **108**, 218703 (2012).
- [8] T. Nepusz and T. Vicsek, *Nat. Phys.* **8**, 568 (2012).
- [9] Y.-Y. Liu, J.-J. Slotine, and A.-L. Barabási, *Proc. Natl. Acad. Sci. (USA)* **110**, 2460 (2013).
- [10] Z.-Z. Yuan, C. Zhao, Z.-R. Di, W.-X. Wang, and Y.-C. Lai, *Nat. Commun.* **4**, 2447 (2013).
- [11] T. Jia, Y.-Y. Liu, E. Csóka, M. Pósfai, J.-J. Slotine, and A.-L. Barabási, *Nat. Commun.* **4**, 3002 (2013).
- [12] D. Delpini, S. Battiston, M. Riccaboni, G. Gabbi, F. Pammolli, and G. Caldarelli, *Sci. Rep.* **3**, 1626 (2013).
- [13] J. C. Nacher and T. Akutsu, *Sci. Rep.* **3**, 1647 (2013).
- [14] G. Menichetti, L. Dall’Asta, and G. Bianconi, *Phys. Rev. Lett.* **113**, 078701 (2014).
- [15] J. Ruths and D. Ruths, *Science* **343**, 1373 (2014).
- [16] S. Wuchty, *Proc. Natl. Acad. Sci. (USA)* **111**, 7156 (2014).
- [17] Z.-Z. Yuan, C. Zhao, W.-X. Wang, Z.-R. Di, and Y.-C. Lai, *New J. Phys.* **16**, 103036 (2014).
- [18] F. Pasqualetti, S. Zampieri, and F. Bullo, *IEEE Trans. Cont. Net. Syst.* **1**, 40 (2014).
- [19] Y.-D. Xiao, S.-Y. Lao, L.-L. Hou, and L. Bai, *Phys. Rev. E* **90**, 042804 (2014).
- [20] F. Sorrentino, *Chaos* **17**, 033101 (2014).
- [21] F.-X. Wu, L. Wu, J.-X. Wang, J. Liu, and L.-N. Chen, *Sci. Rep.* **4**, 4819 (2014).
- [22] A. J. Whalen, S. N. Brennan, T. D. Sauer, and S. J. Schiff, *Phys. Rev. X* **5**, 011005 (2015).
- [23] J. C. Nacher and T. Akutsu, *Phys. Rev. E* **91**, 012826 (2015).
- [24] T. H. Summers, F. L. Cortesi, and J. Lygeros, *IEEE Trans. Cont. Net. Syst.* **3**, 91 (2015).
- [25] Y.-Y. Liu and A.-L. Barabási, *Rev. Mod. Phys.* **88**, 035006 (2016).
- [65] Y.-Z. Chen, L.-Z. Wang, W.-X. Wang, and Y.-C. Lai, *Royal Soc. Open Sci.* **3**, 160064 (2016).
- [66] L.-Z. Wang, Y.-Z. Chen, W.-X. Wang, and Y.-C. Lai, *Sci. Rep.* **7**, 40198 (2017).
- [28] X. F. Wang and G. Chen, *Physica A* **310**, 521 (2002).
- [29] X. Li, X. F. Wang, and G. Chen, *IEEE Trans. Circ. Syst. I* **51**, 2074 (2004).
- [30] F. Sorrentino, M. di Bernardo, F. Garofalo, and G. Chen, *Phys. Rev. E* **75**, 046103 (2007).
- [31] W. Yu, G. Chen, and J. Lü, *Automatica* **45**, 429 (2009).
- [32] B. Fiedler, A. Mochizuki, G. Kurosawa, and D. Saito, *J. Dyn. Diff. Eq.* **25**, 563 (2013).
- [33] A. Mochizuki, B. Fiedler, G. Kurosawa, and D. Saito, *J. Theo. Biol.* **335**, 130 (2013).
- [34] D. K. Wells, W. L. Kath, and A. E. Motter, *Phys. Rev. X* **5**, 031036 (2015).
- [35] L.-Z. Wang, R.-Q. Su, Z.-G. Huang, X. Wang, W.-X. Wang, C. Grebogi, and Y.-C. Lai, *Nat. Commun.* **10**, 11323 (2016).
- [36] J. G. T. Zanudo, G. Yang, and R. Albert, *Proc. Nat. Acad. Sci. (USA)* **114**, 7234 (2017).
- [37] E. Ott, C. Grebogi, and J. A. Yorke, *Phys. Rev. Lett.* **64**, 1196 (1990).
- [38] K. Pyragas, *Phys. Lett. A* **170**, 421 (1992).
- [39] K. Pyragas, *Philos. Trans. Roy. Soc. A* **364**, 2309 (2006).
- [40] W. Lin, *Phys. Lett. A* **372**, 3195 (2008).
- [41] Y. Wu and W. Lin, *Phys. Lett. A* **375**, 3279 (2011).
- [42] H. Ma, D. W. C. Ho, Y.-C. Lai, and W. Lin, *Phys. Rev. E* **92**, 042902 (2015).
- [43] S. P. Bhat and D. S. Bernstein, *SIAM J. Control Optim.* **38**, 751 (2000).
- [44] F. Amato, M. Ariola, and C. Cosentino, *IEEE Trans. Autom. Contr.* **55**, 1003 (2010).
- [45] B. Xu and W. Lin, *Int. J. Bifur. Chaos* **25**, 1550166 (2015).
- [46] H. Rios, D. Efimov, J. A. Moreno, W. Perruquetti, and J. G. Rueda-Escobedo, *IEEE Trans. Autom. Contr.* **PP**, 1 (2017).
- [47] W. Fleming and R. Rishel, *Deterministic and Stochastic Optimal Control* (Springer, New York, 1975).
- [48] See Supplemental Material [url] for analytical estimations of upper bounds for control time and energy cost, data information and convergence times for controlling food-web networks, numerical validation of control flexibility, and realization of finite-time synchronization in coupled spiking neuronal models, which includes Refs. [59–67].
- [49] P. Laslo, C. J. Spooner, A. Warmflash, D. W. Lancki, H.-J. Lee, R. Sciammas, B. N. Gantner, A. R. Dinner, and H. Singh, *Cell* **126**, 755 (2016).
- [50] N. Radde, *Bioinfo.* **26**, 2874 (2010).
- [51] N. Radde, *BMC Syst. Biol.* **6**, 57 (2012).
- [52] J. N. Holland, D. L. DeAngelis, and J. L. Bronstein, *Ame. Nat.* **159**, 231 (2002).
- [53] C. Hui, *Ecol. Model.* **192**, 317 (2006).
- [54] W. C. Allee, O. Park, A. E. Emerson, T. Park, and K. P. Schmidt, *Principles of Animal Ecology*, 1st ed. (W. B. Saunders, London, 1949).
- [55] R. M. May, *Nature* **238**, 413 (1972).
- [56] S. Allesina and S. Tang, *Nature* **483**, 205 (2012).

- [57] M. Ellisa and P. D. Christofides, *Automatica* **50**, 2561 (2014).
- [58] I. Michailidis, S. Baldi, E. B. Kosmatopoulos, and P. A. Ioannou, *IEEE Trans. Auto. Cont.*, Online (2017).
- [59] G. H. Hardy, J. E. Littlewood, G. Pólya, *Inequalities* (Cambridge University Press, Cambridge, 1988).
- [60] W. Rudin, *Functional Analysis* (McGraw-Hill Science, Singapore, 1991).
- [61] V. Lakshmikantham and S. Leela, *Differential and Integral Inequalities* (Academic Press, New York, 1969).
- [62] E. P. Wigner, *Ann. Math.* **67** 325 (1958).
- [63] G. W. Anderson, A. Guionnet, and O. Zeitouni, *An Introduction to Random Matrices* (Cambridge University Press, Cambridge, 2009)
- [64] A.-L. Barabási and R. Albert, *Science* **286**, 509 (1999).
- [65] Y.-Z. Chen and L.-Z. Wang and W.-X. Wang and Y.-C. Lai, *Royal Soc. Open Sci.* **3**, 160064 (2016).
- [66] L.-Z. Wang and Y.-Z. Chen and W.-X. Wang and Y.-C. Lai, *Sci. Rep.* **7**, 40198 (2017).
- [67] J. L. Hindmarsh and R. M. Rose, *Nature* **296** 162 (1982).